Optimizing Electrical Energy Dispatch in Goma (DRC) Using Artificial Neural Networks

Kambale Pawase Gershome[1], Baraka Mushage Olivier[2], Twizere Bakunda J. Daudet[3], Tsochounie Jules Hubert[4]

[1]Departement of Sciences and Technology, La Sapientia Catholic University of Goma, Goma, Democratic Republic of Congo
Email: *gershwmpawase[at]gmail.com*

[2]Departement of Sciences and Technology, the Université Libre des Pays des Grands Lacs de Goma, Goma, Democratic Republic of Congo
Email: *Olivermushage[at]gmail.com*

[3]Departement of Applied Sciences, the Institut Superieur de Technique Appliquée de Goma, Goma, Democratic Republic of Congo
Email: *twizdau[at]gmail.com*

[4]Departement of Sciences and technology, Université des Montagnes, Gangangte, Republic of Cameroon
Email: *jhtsoch[at]gmail.com*

Abstract: ***This study addresses the growing electricity demand in Goma, DRC, amidst limited energy resources. By integrating Artificial Neural Networks (ANNs) with optimization techniques, the research proposes an interconnection network to enhance resource sharing and improve forecasting for electricity production and demand. The ANN model achieved 90% accuracy in energy distribution, reducing computation time and optimizing costs. Results underscore the critical role of resource management and policy reforms in ensuring sustainable energy solutions.***

Keywords: Optimal dispatch, power flow optimization, Artificial Neuronal Networks, energy management, electricity distribution

1. Introduction

Energy is a cornerstone of national development, serving as the driving force behind industrialization and the foundation for nearly all human activities and services. It is essential for production, transportation of people and goods, raw material processing, and trade.

To be utilized, primary energy—such as coal, natural gas, oil, solar, and wind—must be converted into various forms, with electrical energy being the most widely used. Since the 1970s, research has demonstrated a direct correlation between electrical energy consumption and a nation's gross domestic product (GDP), highlighting its critical role in overall and sectoral economic growth. [1]. Consequently, the stability and availability of electrical energy are intrinsically linked to a country's GDP and overall economic development.

Goma, situated in the eastern Democratic Republic of Congo, faces a critical energy crisis. As of 2023, the city had an estimated population of 2.3 million, with an electricity demand of 55 MW—far surpassing the available supply of approximately 19.9 MW. This limited supply is shared among four main providers: SNEL (8 MW), Virunga Énergie (5.6 MW), NURU (1.3 MW), and SOCODEE, which distributes 5 MW sourced from Virunga Énergie [2] [3]. This shortage results in an electricity access rate of less than 50%, negatively impacting the quality of basic services and hindering the city's socio-economic development. Furthermore, the independent operation of energy providers exacerbates the instability and low reliability of the electrical grid.

To address Goma's energy challenges, several projects have been proposed, including the construction of the MATEBE 2 hydroelectric power plant at RWANGUBA, the interconnection of SNEL with the NELSAP community, and the development of the NURU 2 solar power plant. These initiatives aim to meet the growing electricity demand and improve the quality of life for the city's residents.

Despite these efforts, Goma continues to face significant challenges due to limited electricity sources. This article proposes a strategy for the economic distribution of electrical energy to ensure a reliable, high-quality energy supply in sufficient quantities, while optimizing costs and minimizing losses. The proposed strategy relies on production and demand forecasts and includes:

- A neural network to predict energy demand;
- Neural networks to forecast power plant production;
- A multilayer perceptron for economically allocating demand, accounting for production unit constraints and enabling a five-hour forecast.

The primary objective of this paper is to optimize energy management in Goma by leveraging advanced technical and economic solutions.

The article presents a comprehensive literature review of prior research on load distribution optimization using various methodologies. It outlines the study's context, details the adopted methodology, and provides an analysis and interpretation of the results. Finally, it evaluates the effectiveness of the proposed optimization method by comparing it with classical approaches.

2. Literature Review

The use of artificial neural networks in the field of energy and electrical grids is extensive and diverse. These networks are employed to address issues related to reliability, security, optimization, stability, and safety. In the area of optimization, numerous researchers have explored various aspects and techniques incorporating artificial intelligence.

Miodrag et al. in their study propose a hybrid method that combines artificial neural networks with an iterative approach. Utilizing a multilayer perceptron trained via gradient descent to predict the penalty factor, the method significantly reduces computation time from 31.5 seconds to 1.08 seconds while ensuring high accuracy in the optimal distribution of contributions from production units [4].

Kumar et al. in their study propose to use artificial neural networks to enhance efficiency and reduce computation time. The results demonstrate a 50% reduction in computation time with an accuracy of 1%, outperforming classical methods [5].

Naama et al. propose a hybrid method that combines a genetic algorithm with a Newtonian analytical method to optimize power distribution in an electrical network. Artificial intelligence is employed for lossless optimization, while the Newton-Raphson method is used to calculate losses. Simulation results demonstrate that this hybrid approach is more efficient, faster, and more robust than using either method alone, providing satisfactory outcomes in terms of both speed and accuracy [6].

Syai'in et al. in their propose an Optimal Power Flow (OPF) method using an artificial neural network trained with data derived from the classical particle swarm optimization method. The results indicate a deviation of only 0.12% between the predicted and actual values, along with faster execution compared to the classical approach [7].

Mountassir et al. propose the use of artificial neural networks to predict energy demand in smart electrical grids. Considering energy consumption as a nonlinear time series problem, they adopt the CRBM (Conditional Restricted Boltzmann Machine) method, a stochastic machine learning model. The results show that this method can predict the energy consumption of an office building over a week with hourly resolution, surpassing advanced methods like ANN, due to its probabilistic power [8].

Kadir et al. study a method for solving the power flow problem based on a multilayer perceptron, combined with a differential optimization algorithm to generate training data. The results show that this approach effectively solves static, dynamic, and complex power flow problems without resorting to traditional iterative methods. It can also be used for the dynamic optimization of power flow, control, and fault prediction, without requiring simulations or complex software that is costly in terms of resources or time [9].

The research highlights a convergence in using artificial neural networks (ANNs), often integrated with hybrid approaches, to optimize the production and distribution of electrical energy. These methods, built on multi-layer perceptron, are combined with techniques such as genetic algorithms (Naama et al., 2007), the Newton-Raphson method (Naama et al., 2007), particle swarm optimization (Syai'in et al., 2010), differential algorithms (Kadir et al., 2019), and gradient descent approaches (Miodrag et al., 1996). Classical optimization methods are frequently employed to generate training data.

This paper employs a combination of advanced optimization techniques and neural network models. The Kuhn-Tucker method is used to generate optimization data, while the Gauss-Seidel method assesses network losses. Optimal power flow minimizes electricity production costs and system constraints by optimizing unit contributions and reducing losses. The KRON-based B-coefficient method calculates power losses. For forecasting, the study uses LSTM networks with a many-to-many architecture to predict solar power production and electricity demand based on 48-hour historical data. A multilayer perceptron addresses optimal demand distribution, adhering to production limits and constraints. The methodology also adopts synchronous interconnection for stable operation, resource sharing, and enhanced reliability, leveraging identical production source frequencies and automatic control mechanisms.

The results demonstrate significant improvements in computation time and accuracy: computation time reductions of up to 50% (Kumar et al., 1995) or down to 1.08 seconds (Miodrag et al., 1996), with minimal prediction errors, such as a deviation of only 0.12% (Syai'in et al., 2010). These hybrid methods also exhibit greater robustness and adaptability to complex problems, such as predicting non-linear time series (Mountassir et al., 2018) or dynamically optimizing power flow (Kadir et al., 2019).

3. Methodology

The following are the approaches and tools used in this paper.

3.1 Description of Goma's Electrical Infrastructure

Electricity plays a central role in sustainable development, impacting both economic recovery and industrialization. The city of Goma is powered by the public utility SNEL and private companies: Virunga Energie, NURU, and SOCODEE.

- **SNEL** provides 8 MW of electricity to Goma from the Ruzizi hydroelectric plant near Bukavu via a high-voltage (HV) line of 75 kV, reduced to 70 kV at Goma [10]. The company plans to import 70 MVA from Ethiopia through the NELSAP project.
- **Virunga Energie**, affiliated with the Congolese Institute for Nature Conservation (ICCN), produces 12.6 MW from the Matebe power plant, delivering 5.6 MW to Goma via a 33 kV line. An ongoing electrification project includes the construction of the Rwanguba plant (28 MW) to meet the growing demand.
- **NURU SARL** operates a hybrid solar power plant with a capacity of 1.3 MW in the Ndosho neighborhood, distributing electricity at 11 kV. Additionally, NURU is constructing the **NURU 2** plant in the Lac-Vert neighborhood, with a projected capacity of 3.8 MW, to further meet increasing demand.

International Journal of Science and Research (IJSR)
ISSN: 2319-7064
Impact Factor 2024: 7.101

- **SOCODEE** manages a 33 kV distribution network and rents 5 MW from Virunga Energie to supply Goma.

With a rapidly increasing energy demand estimated at 55 MW [3], this growth is driven by accelerated urbanization and Goma's attractiveness due to its economic development and migration from conflict-affected areas.

The city of Goma has an installed load of 91.9 MVA, distributed across four main networks: SNEL (53.6%), Virunga Energie (20.1%), SOCODEE (24%), and NURU (2.3%). Figure 1 presents a map of these networks in Goma, with a background showing the DRC map and North Kivu province highlighted in blue.

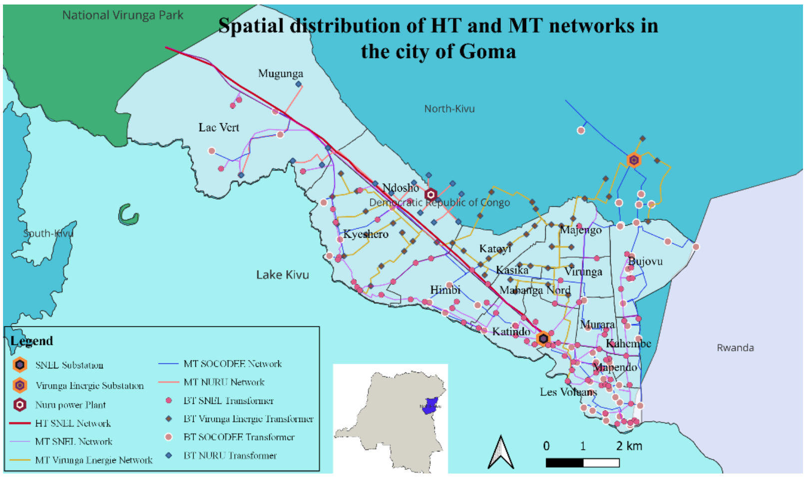

Figure 1: Spatial distribution of HT and MT networks in Goma

3.2 Data Collection and Processing Tools

This study investigates the use of artificial neural networks to optimize the distribution of electrical energy in Goma, with the goals of optimizing production resources and standardizing the cost per kilowatt for subscribers. It presents a method for forecasting demand and production over a 5-hour time horizon, utilizing data collected from energy companies and online databases, such as Kaggle.

For optimization, the data will be generated using the **Kuhn-Tucker** method [11], and network losses will be assessed with the **Gauss-Seidel** method. Time-series forecasting will be performed using LSTM neural networks, while a perceptron will address the optimization challenges. Interconnecting the networks is a crucial step in achieving this objective.

Python (via ANACONDA) will be employed for data analysis, design, and testing, while ETAP 19 will be used for modeling the power grid.

3.3 Power grid interconnection

The interconnection of electrical networks can be synchronous, requiring identical frequencies (50 Hz or 60 Hz), or asynchronous, operating with either identical or different frequencies. The most used method is synchronous interconnection, which connects networks via an AC connection line and ensures stable operation through automatic generator control and power flow management devices [12]. The interconnection enhances flexibility, resource sharing, and network reliability. In this study, the synchronous method will be adopted due to the identical frequencies of the production sources.

3.4 Optimum Power Flow

Optimal power flow aims to minimize the cost of electricity production while respecting the constraints of the network and equipment. This method optimizes the contribution of each production unit, reduces losses in the lines, penalizes costly or inefficient units, and limits the environmental impact. The objective is achieved by minimizing a function related to production cost [13]. The cost function is given by formula (1).

$$C_t = \sum_{i=1}^{n} C_i \tag{1}$$

C_i is the production cost of the generator unit i. The cost of production can be influenced by factors such as resource availability, maintenance costs, generator performance, line losses, market conditions, investment costs, capital, and generated power, typically represented by a second-order polynomial, as given in formula (2).

$$C_i = \alpha_i + \beta_i P_i + \gamma_i P_i^2 \tag{2}$$

P_i is the production power of unit i. The power plants are constrained by their minimum and maximum production limits, as shown in equation (3), and must meet the demand plus network losses, in compliance with the equality constraint defined in equation (4).

$$P_{imin} \leq P_i \leq P_{imax} \tag{3}$$

$$\sum_{i=1}^{n} P_i - P_D - P_L = 0 \tag{4}$$

P_D and P_L represent the power demand and network losses, respectively.

To optimize the distribution of electrical energy while accounting for equality and inequality constraints, the Kuhn-Tucker iteration method is employed. This method is based on the Lagrange equation, as presented in equation (5).

$$L = C_t + \lambda\left(P_D + P_L - \sum_{i=1}^{n} P_i\right) \tag{5}$$

λ is the Lagrange multiplier, and the minimum of the function is achieved when its partial derivatives are equal to zero, leading to equation (6).

$$\begin{cases} \dfrac{\partial L}{\partial P_i} = 0 \\ \dfrac{\partial L}{\partial \lambda} = 0 \end{cases} \Rightarrow \begin{cases} \lambda = \dfrac{\partial C_i}{\partial P_i}\left(\dfrac{1}{1 - \dfrac{\partial P_L}{\partial P_i}}\right) \\ P_L + P_D = \displaystyle\sum_{i=1}^{n} P_i \end{cases} \tag{6}$$

The power losses caused by the transit of the generated power P_i in the network are determined using the KRON method, adopted by KIRCHMAYER, and referred to as the B-coefficient method [11] [14]. This method evaluates the power flow within the network. The simplest formula can be used when exchanges between upstream networks are minimal. It is calculated using equation (7).

$$P_L = \sum_{i=1}^{n} B_{ii} P_i \tag{7}$$

The coefficient B_{ii} can be calculated by determining the partial derivative of the loss function with respect to the generated power, as defined in equation (8).

$$B_{ii} = \frac{1}{2P_i}\frac{\partial P_L}{\partial P_i} \tag{8}$$

The power contribution for a power plant will then be calculated using equation (9).

$$P_i = \frac{\lambda - \beta_i}{2\left(\gamma_i + \lambda B_{ii}\right)} \tag{9}$$

After calculating the contribution of each source, the equality and inequality constraints must be verified. If any constraint is violated, λ must be updated, and a source's contribution will be set to its maximum if its production exceeds the maximum limit [11]. The errors on the equality constraint and on λ are then defined according to equation (10).

$$\begin{cases} \Delta P^{k-1} = P_D + P_L^{k-1} - \displaystyle\sum_{i=1}^{n} P_i^{k-1} \\ \lambda^k = \lambda^{k-1} + \Delta\lambda^{k-1} \end{cases} \tag{10}$$

The variation of λ is computed using a Taylor series expansion of the Lagrange function's partial derivative, as expressed in equation (11).

$$\Delta\lambda^{k-1} = \frac{\Delta P^{k-1}}{\displaystyle\sum_{i=0}^{n}\left(\frac{\partial P_i}{\partial \lambda}\right)^{k-1}} \tag{11}$$

$$\sum_{i=1}^{n}\left(\frac{\partial P_i}{\partial \lambda}\right)^{k-1} = \sum_{i=1}^{n}\frac{\gamma_i + B_{ii}\beta_i}{2\left(\gamma_i + \lambda B_{ii}\right)^2}$$

The optimal power flow algorithm using the Kuhn-Tucker method is executed as illustrated in the flowchart shown in Figure 2.

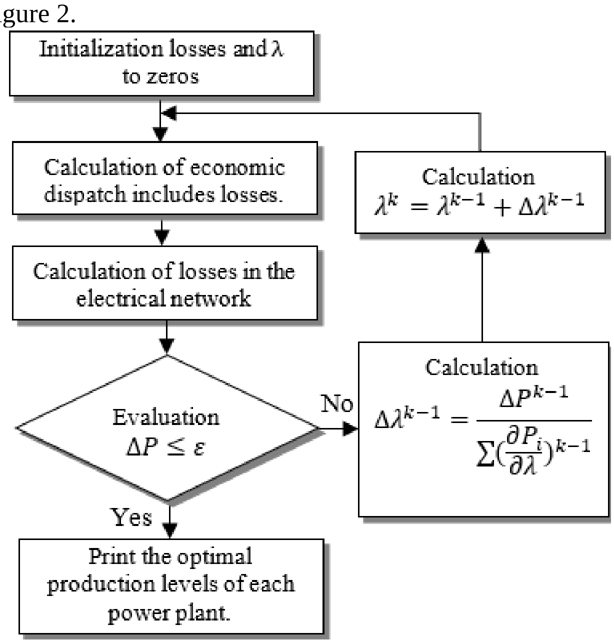

Figure 2: OPF Algorithm using Kun-Trucker method

3.5 Gauss-Seidel method

The Gauss-Seidel method is an iterative technique used in electricity to solve power flow problems. In this work, it is employed to determine voltages or active and reactive powers at buses, enabling the calculation of network losses [11]. Equation (12) presents the voltages at the buses, while equation (13) represents the powers.

$$v_i^{k+1} = \frac{\dfrac{P_i + jQ_i}{v_i^{*(k)}} + \sum y_{ij} v_j^{(k)}}{\sum y_{ij}}, \quad i \neq j \tag{12}$$

$$\begin{aligned} P_i^{(k+1)} &= Real\left(v_i^{*(k)}\left(v_j^{(k)}\sum y_{ij} - \sum y_{ij} v_j^{(k)}\right)\right), \quad i \neq j \\ Q_i^{(k+1)} &= Imag\left(v_i^{*(k)}\left(v_j^{(k)}\sum y_{ij} - \sum y_{ij} v_j^{(k)}\right)\right), \quad i \neq j \end{aligned} \tag{13}$$

i and j: indices of the buses; P_i: active power at bus i; Q_i: reactive power at bus i; y_{ij}: admittance between bus i and bus j; $v_i^{*(k)}$ conjugate of the voltage at bus i during iteration k. $v_j^{(k)}$: voltage at bus j during iteration k.

After solving the power flow equations, the losses in the network can be calculated. The losses between two buses i and j are the sum of the complex powers S_{ij} transmitted from bus

i to bus j and S_{ji} transmitted from bus j to bus i, as given by equation (14).

$$S_{Lij} = S_{ij} + S_{ji} \tag{14}$$

3.6 Recurrent Neural Network

A recurrent neural network (RNN) is a type of neural network designed to process sequential data or time series. RNNs process each element of a sequence successively, maintaining a hidden state that acts as a memory of past information. At a given time t, the outputs of the hidden cells depend on their outputs at the previous time $(t-1)$, allowing distant events in time to be connected [15].

Long Short-Term Memory networks (LSTMs), an advanced variant of Recurrent Neural Networks (RNNs), address the challenge of vanishing or exploding gradients by enabling the effective learning and retention of long-term dependencies. Unlike traditional RNNs, LSTMs distinguish between short-term information, represented by the hidden state, and long-term information, encapsulated in the cell state. Figure 3 illustrates the architecture of a standard LSTM cell, which includes a forget gate to regulate the retention and disposal of information. The system of equations (Equation 15) describes the mathematical relationships governing the interactions between the various components of the LSTM cell [15].
This research uses LSTM networks with a many-to-many architecture to predict 5-hour solar production of Photovoltaic (PV) power plant and electricity demand in Goma, based on the previous 48 hours of data.

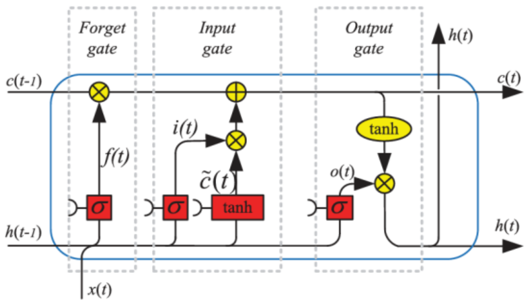

Figure 3: LSTM cell with a forget gate [15]

$$\begin{aligned}
f_t &= \sigma\left(W_{fh}h_{t-1} + W_{fx}x_t + b_f\right)\\
i_t &= \sigma\left(W_{ih}h_{t-1} + W_{ix}x_t + b_i\right)\\
\tilde{C}_t &= \tanh\left(W_{\tilde{c}h}h_{t-1} + W_{\tilde{c}x}x_t + b_{\tilde{c}}\right)\\
C_t &= f_tC_{t-1} + i_t\tilde{C}_t\\
O_t &= \sigma\left(W_{oh}h_{t-1} + W_{ox}x_t + b_o\right)\\
h_t &= O_t\tanh\left(C_t\right)
\end{aligned} \tag{15}$$

3.7 Multilayer perceptron

The multilayer perceptron is a widely used neural network where data flows from input to output without feedback. It is used to create complex nonlinear mathematical functions [16]. In this research, it will be employed to solve the optimal demand distribution problem, considering production limits while respecting the equality constraint. Figure 4 illustrates a perceptron with two hidden layers, each containing five neurons, two input neurons, and one output neuron.

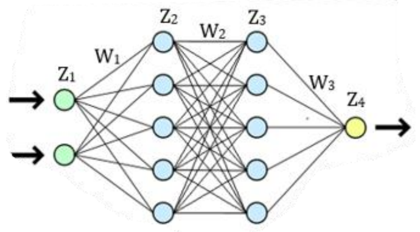

Figure 4: Multilayer perceptron

For a perceptron with n layers, each composed of neurons with an activation function f, if $Z_1, Z_2, \ldots Z_n$ are the input data matrices for layers $1, 2, ..n$, $W_1, W_2, \ldots W_n$ are the weight matrices, and $b_1, b_2, \ldots b_n$ are the bias matrices, then the output matrix Z_y is defined by equations (16).

$$\begin{aligned}
Z_2 &= f\left(Z_1W_1 + b_1\right)\\
Z_3 &= f\left(Z_2W_2 + b_2\right)\\
&\ldots\\
Z_y &= f\left(Z_nW_n + b_n\right)
\end{aligned} \tag{16}$$

3.8 Training Artificial Neural Networks

In this study, neural networks are used to predict the future production of each unit, energy demand, and the optimal contribution of sources for the next five hours. An LSTM sequence-to-sequence model, followed by a multilayer perceptron, is employed to analyze historical data and forecast over a 5-hour. The Adam optimizer was chosen for its efficiency in deep learning tasks. Training involves forward propagation, error calculation using the Mean Squared Error (MSE) function, presented in Equation (17), and backpropagation to update the network's parameters.

$$MSE = \frac{\sum_{i=0}^{n}\left(Y_i - \bar{Y}_i\right)^2}{n} \tag{17}$$

$\underline{Y}_i$: the true value;

Y_i : the predicted value;

n : the total number of pairs $\left(Y_i, \bar{Y}_i\right)$

4. Results

4.1 Design of the interconnection network

The interconnection network aims to facilitate energy exchange between systems, optimize costs and resources, and enhance reliability, stability, and flexibility. It utilizes existing distribution lines, including sources such as NURU 2, Rwanguba for Virunga Energy, and NELSAP for SNEL. The interconnection is carried out at 33 kV, with the substation located at Mugunga. Figure (5) illustrates the location of the interconnection substation on the map, while Figure (6) presents the principle of the interconnection network.

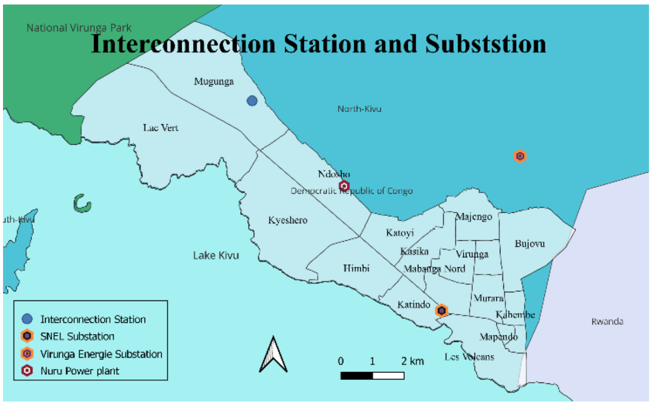

Figure 5: Location of interconnection station and substation

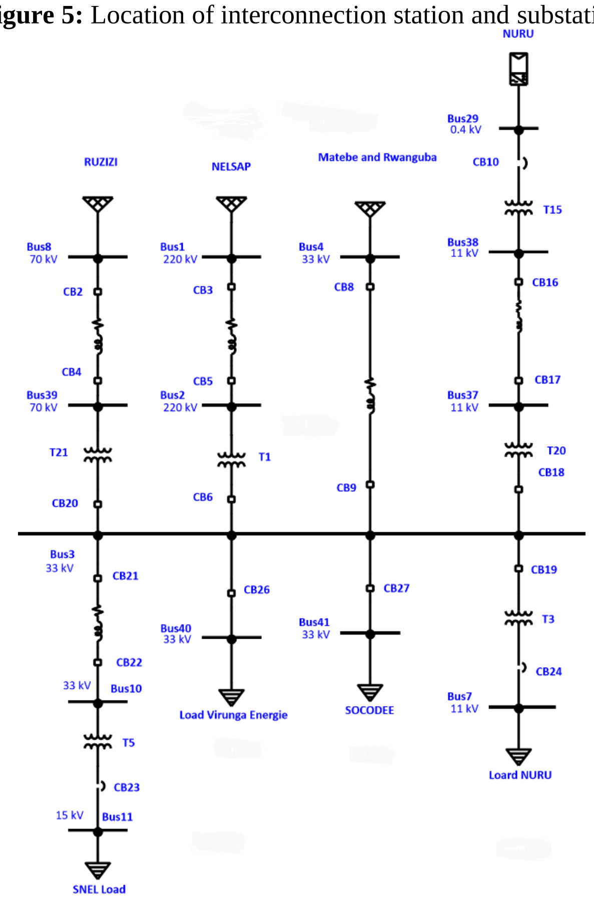

Figure 6: Interconnection network

The transformers will be considered ideal. To simplify the power flow study in this network, it is essential to adapt the transformer connections into a π-structure model.

The Nuru-Interconnection Station line, 4 km long, will be sized for a maximum power of 6.6 MW, corresponding to 75% utilization of its capacity. Considering 8% losses of voltage, 95% efficiency, a power factor of 0.85, and a voltage of 11 kV, its characteristics are calculated using equation (18).

$$R = \rho \frac{l}{s}$$

$$L = \frac{\Delta V - RI\cos\varphi}{2\pi f\, I\sin\varphi} \tag{18}$$

$$D = \frac{0.779r.e^{\frac{L''}{2.10^{-7}}}}{\sqrt[3]{2}}$$

The Nuru-Interconnection Station line is defined by a cable cross-section of 185 mm² and a phase-to-phase spacing of 1 meter.

The characteristics of the interconnection network are presented in Table 1.

Table 1: Interconnection networks characteristics

Characteristics \ Power Plant	*SNEL*	*Virunga Energie/ SOCODEE*	*NURU*	*NELSAP (project)*
Maximum Power (MW)	12	10	1.3	100
Minimum Power (MW)	3	0	0	0
Installed Load (MW)	49,3	40,5	2,1	-
Power Factor	0,85	0,85	0,85	-
Project (MW)	-	28	3,7	-
Transmission Line Length (Km)	136,5	79	4	93
Transmission Line Section (mm2)	70	148	185	2x70
Distance between cables (m)	2	1.5	1	3
cable material	ALAC	ALMELEC	ALAC	ALAC
Cable arrangement	flag	flag	vault	flag
Transmission voltage (kV)	70	33	11	220
Repartition Voltage (kV)	15	33	11	-

5.2 The prediction of electrical energy demand

The primary objective of this work is to design a neural network capable of predicting electrical energy demand. This demand can fluctuate based on various factors, including weather conditions, time of day, GDP, kilowatt-hour price, and more. In this research, demand prediction is primarily based on variables such as time, date, and day type (weekday

Paper ID: SR25120191055 DOI: https://dx.doi.org/10.21275/SR25120191055

or weekend). Figure 7 illustrates the correlation between these factors and energy demand.

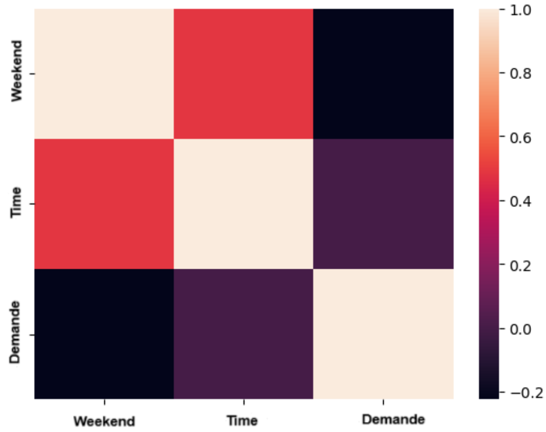

Figure 7: Electricity demand correlations.

Figure 7 indicates a moderate correlation between demand and the hour of the day, and a weak correlation between demand and whether it is a weekend or not. Therefore, the prediction of demand based on historical demand associated with the date is carried out using the ANN model presented in Table 2.

Table 2: ANN model for demand prediction

LAYER (TYPE)	*OUTPUT SHAPE*	*PARAM #*
LSTM_1 (LSTM)	(None, 48, 64)	17408
LSTM_2 (LSTM)	(None, 64)	33024
DENSE_1	(None, 128)	8320
DENSE_2	(None, 3)	387
TOTAL PARAMS: 59139 (231.01 KB) *TRAINABLE PARAMS: 59139 (231.01 KB)* *NON-TRAINABLE PARAMS : 0 (0.00 BYTE)*		

The model presented in Table 2 uses a sequence of 48 input data, processed by two LSTM layers and a two-layer perceptron for the output. It contains 59,139 trainable parameters and uses the "elu" activation function. The training, carried out in 12 minutes over 5 iterations and 3,633 data batches, aims to capture temporal dependencies and perform a final regression. The training curve is illustrated in Figure 8.

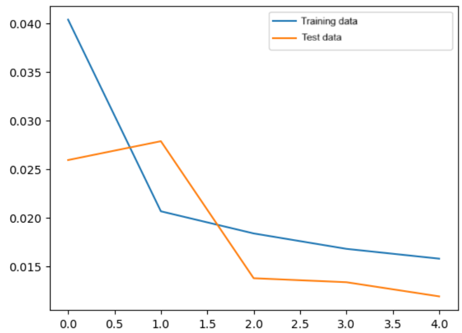

Figure 8: Training curve of electricity demand predict.

Figure 8 shows a gradual reduction in prediction error, with an MSE of 0.015 for training data and 0.011 for test data after 5 iterations, indicating that the model effectively captures temporal relationships. Figure 9 illustrates the predictions over a five-hour sequence, comparing actual demand (blue curve) with predicted demand (red curve).

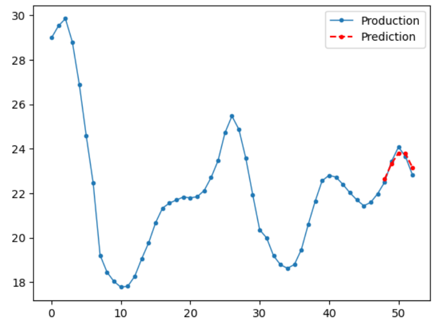

Figure 9: Prediction curve of electricity demand.

Figure 9 shows the model's performance in predicting electrical energy demand, with a maximum error of 1.43% compared to the actual demand.

5.3 The prediction of PV production

A photovoltaic solar power plant converts solar energy into electricity, with its production influenced by meteorological factors such as temperature and irradiation. The production dataset includes measured electric power, ambient temperature, module temperature, irradiation, and time. The correlation between these variables is analyzed, as shown in Figure 10.

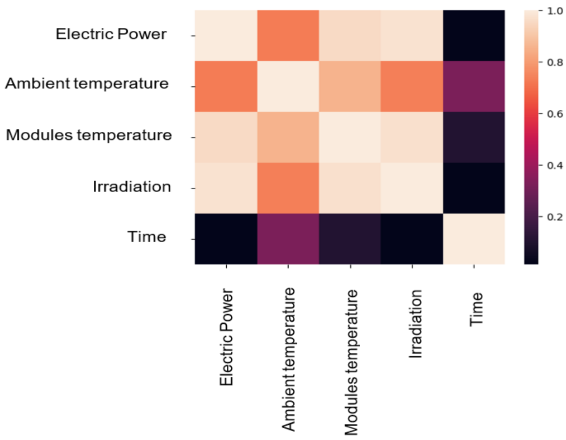

Figure 10: Correlation among PV production variables

Figure 10 highlights a strong correlation between the power produced and irradiation, a significant correlation with module temperature. A moderate correlation is observed with ambient temperature, while time shows a weak correlation with other variables. Consequently, a neural network model based on LSTM layers and dense layers, as described in Table 3, will be used to predict future production by considering past data and weather history.

Table 3: ANN model for production PV prediction

LAYER (TYPE)	*OUTPUT SHAPE*	*PARAM #*
LSTM_1 (LSTM)	(None, 48, 100)	42400
LSTM_2 (LSTM)	(None, 48, 64)	42240
LSTM_3 (LSTM)	(None, 32)	12416
DENSE_1 (DENSE)	(None, 128)	4224
DENSE_2 (DENSE)	(None, 32)	4128
DENSE_3 (DENSE)	(None, 5)	165
TOTAL PARAMS: 105573 (412.39 KB) *TRAINABLE PARAMS: 105573 (412.39 KB)* *NON-TRAINABLE PARAMS : 0 (0.00 BYTE)*		

The model presented in Table 3 processes an input sequence of 48 time-series data, passing through multiple layers: 100, 64, and 32 LSTM modules, followed by a three-layer perceptron with 128, 32, and 5 neurons. It has 105,573 trainable parameters and utilizes the "elu" activation function. The training, conducted over 8 iterations with 422 batches of size 32, takes around 6.37 minutes. The training curves are shown in Figures 11.

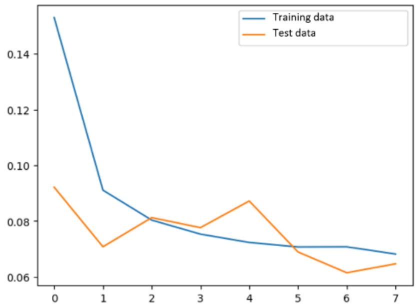

Figure 11: Training curve of PV production predict

The graph in Figure 11 shows a continuous decrease in prediction error. After 8 iterations, the mean squared error is 0.068 for the training data and 0.064 for the test data, reflecting a very low learning error. This indicates that the model has effectively captured the relationships between meteorological data and the production of a photovoltaic power plant. Figure 12 presents the photovoltaic production forecasts over a five-hour period: the blue curve represents the actual production, while the red curve shows the predicted values.

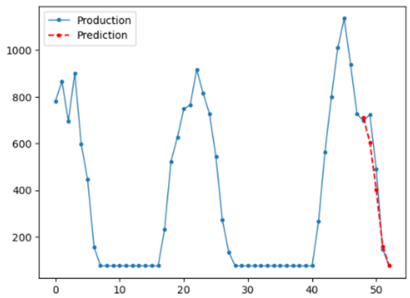

Figure 12: Prediction curve of PV production.

Figure 12 shows the model's performance in predicting electrical production of PV, with a maximum error of 9.9% compared to the actual production.

5.4 The economic load dispatch

Economic dispatch involves optimally allocating the demand for electrical energy among power plants, minimizing production costs and network losses while adhering to equality and inequality constraints. For this work, the main object is to optimize production costs in real-time using neural network models. It relies on an ANN trained using the Kuhn-Tucker method.

5.4.1 Cost function

The cost function is quadratic in form. For SNEL, the average price for distribution is $ 0.078/kWh, representing the linear production coefficient [17]. We will consider NELSAP's production cost to be identical to that of SNEL, and for Nuru, a cost proportional to production. Some billing details are presented in Table 4.

Table 4: Some distributions bill [17] [18]

Power Plants	*Price ($)*	*Energy (KWh)*
Virunga Energie / SOCODEE	270	1082,1
	50	200,4
	300	1202,3
SNEL / NELSAP	0,0888	1
	10	96
NURU	0,4	1

The resolution of the cost function (Equation (2)) using the data from Table 4 allows for determining the cost function of Equation (19).

$$C_t = 31.93 + 249.43P_{Vir} + 78(P_{NEL} + P_{SNEL}) + 400P_{Nuru} + 0.27(P^2_{NEL} + P^2_{SNEL}) + 0.000062P^2_{Vir} \quad (19)$$

P_{vir} : the production of the Matebe power plants.
P_{Nuru} : the production of Nuru power plants
P_{SNEL} : Goma's quota of the Ruzizi power plants' production.
P_{NEL} : Goma's quota of NELSAP line

The function in Equation (17) indicates a linear increase in total production cost of 400, 78, 249.43, and 78 for each additional 1 MWh from the Nuru, Ruzizi, Matebe, and NELSAP sources, respectively, with fixed costs of approximately 31.93$/h.

5.4.2 Optimization of production costs

The function to be optimized is the cost function. The problem formulation is built around the Lagrange equation (20).

$$L = C_t + \lambda(P_D + P_L - P_{Vir} - P_{NEL} - P_{SNEL} - P_{Nuru}) \quad (20)$$

The dynamic equality and inequality constraints are given in Equations (21) and (22).

$$P_D + P_L - P_{Vir} - P_{Nuru} - P_{SNEL} - P_{NEL} = 0 \quad (21)$$

$$\begin{aligned} P_{Nurumin} &\le P_{Nuru} \le P_{Nurumax} \\ P_{Virmin} &\le P_{Vir} \le P_{Virmax} \\ P_{SNELmin} &\le P_{SNEL} \le P_{SNELmax} \\ P_{NELmin} &\le P_{NEL} \le P_{NELmax} \end{aligned} \quad (22)$$

The iterative Kuhn-Tucker method generated a dataset with 1,524 entries to train the artificial neural network. Each entry details the inequality constraints of each power plant, the demand, and the outputs to economically meet the demand. Correlations between these variables are shown in Figure 13.

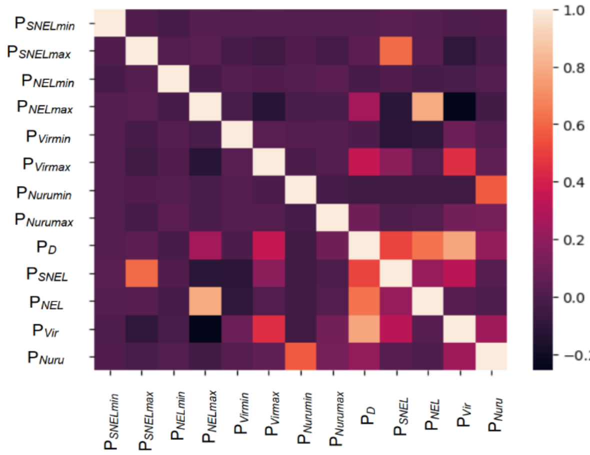

Figure 13: Correlation among economic dispatch variables

Figure 13 indicate a strong correlation between power plant outputs and demand, as production must meet demand. Virunga Energie (Matebe) shows the highest correlation (~0.8), followed by NELSAP (~0.7), SNEL (Ruzizi) (~0.5), and the solar plant Nuru (~0.2). These differences are due to variations in production costs, availability, and losses during production and transport. Nuru is most affected by its high production cost, while Ruzizi faces challenges from transport losses and limited availability.

Correlations between outputs and constraints indicate that low-cost plants operate near their maximum limits: NELSAP (~0.85), SNEL (~0.7), and Matebe (~0.5). Meanwhile, Nuru's production is strongly tied to its lower limit (~0.65).

To predict optimal outputs for each unit based on demand and production constraints, a simple neural network model will be used, as detailed in Table 5.

Table 5: ANN model for economic dispatch prediction

LAYER (TYPE)	*OUTPUT SHAPE*	*PARAM #*
DENSE_1 (DENSE)	(None, 16)	160
DENSE_2 (DENSE)	(None, 32)	544
DENSE_3 (DENSE)	(None, 16)	528
DENSE_4 (DENSE)	(None, 4)	68
TOTAL PARAMS: 1300 (5.08 KB) TRAINABLE PARAMS: 1300 (5.08 KB) NON-TRAINABLE PARAMS: 0 (0.00 BYTE)		

The model is a multilayer perceptron with 16 input neurons connected to a 9-dimensional input vector. These 16 neurons are fully connected to 32 neurons, followed by 16 neurons fully connected to 4 output neurons, representing the power plant outputs. The network has 1,300 trainable parameters and uses the "ReLU" activation function.

Training consists of 50 iterations on a dataset of 1,219 samples, grouped into batches of size 16, taking approximately 111 milliseconds. The precision error training curve is shown in Figure 14.

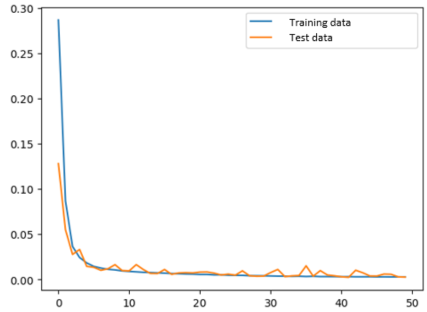

Figure 11: Training curve of PV production predict.

The curve in Figure 4 shows a gradual decrease in error. After 50 iterations, the prediction error is approximately 0.0029 for the training data and 0.0026 for the test data, corresponding to an accuracy of 98.2% for training data and 90% for test data. Table 6 presents an evaluation of the model on 5 samples compared to the classical method. Each row describes the inequality constraints of the production units, the demand, the optimal dispatch according to the classical method and the predictions, along with the average error

Table 6: Testing the ANN model for predicting dispatch considering the dynamics of demand and production units.

		Inequality constraints				Demand (MWh)	***Optimum dispatch***					Average Error (%)
		SNEL (MWh)	NELSAP (MWh)	Virunga Energie (MWh)	Nuru (MWh)			SNEL (MWh)	NELSAP (MWh)	Virunga Energie (MWh)	Nuru (MWh)	
1	*Min*	1.59	0.984	0.2	0.91	29.76	Real	6.989	9.065	16.17	0.919	1.32
	Max	6.98	9.065	28.1	1.17		Predict	7.890	9.136	16.53	0.510	
2	*Min*	0.101	0.949	2.65	0.54	45.05	Real	7.148	15.94	27.21	0.542	0.63
	Max	7.14	15.94	37.8	2.94		Predict	8.086	16.25	27.23	0.565	
3	*Min*	1.016	1.517	2.75	0.63	51.23	Real	8.649	29.35	16.6	0.637	0.71
	Max	8.64	29.35	32.19	4.70		Predict	9.662	29.76	16.75	0.629	
4	*Min*	2.36	0.826	1.039	0.12	40.98	Real	7.198	25.47	10.93	0.123	1.14
	Max	7.19	25.47	30.88	0.83		Predict	8.237	25.68	10.52	0.467	
5	*Min*	2.79	3.326	1.81	0.85	30.11	Real	5.894	23.12	1.81	0.854	0.99
	Max	8.90	24.57	37.23	1.27		Predict	6.330	23.35	1.472	0.592	

Table 16 shows a maximum error of 1.32% across five samples, demonstrating that the model effectively learned the economic dispatch of electrical energy, making it possible to replace the classical Kuhn-Tucker method with 90% accuracy.

5.5 Evaluation of the Method Set

In this evaluation, we measure the losses generated by the method using artificial intelligence compared to the classical method, as well as the time required for optimization. The five future productions and demands are predicted with fixed limits. The results of this evaluation are presented in Table 7 and table 8.

Paper ID: SR25120191055 DOI: https://dx.doi.org/10.21275/SR25120191055

Table 7: Evaluation of the ANN optimization model considering static productions

NO.		Demand (MW)	Optimum dispatch (MW)				Times (ms)	Losses (MW)	Production costs ($/H)
			SNEL	NELSAP	Virunga Energie	Nuru			
1.	*Real*	25.713	4.347	16.893	5	1	151.8	1.53	3417.95
	Predict	25.752	4.645	17.516	5.436	0.648	25	1.606	3464.25
2.	*Real*	27.427	4.70	18.309	5	1	126.23	1.58	3570.25
	Predict	27.425	5.024	18.719	5.24	0.509	26	1.64	3495.92
3.	*Real*	28.709	4.964	19.369	5	1	121.7	1.62	3685.02
	Predict	28.760	5.277	19.554	5.017	0.39	23	1.65	3488.89
4.	*Real*	29.572	5.142	20.084	5	1	167.25	1.65	3762.75
	Predict	29.805	5.475	20.207	4.8395	0.305	30	1.67	3482.58
5.	*Real*	30.235	5.278	20.634	5	1	126.8	1.67	3822.69
	Predict	30.596	5.586	20.773	4.760	0.293	30	1.68	3517.35

Table 8: Evaluation of the ANN optimization model considering SNEL and NELSAP as highly constrained

NO.		Demand (MW)	Optimum dispatch (MW)				Times (ms)	Losses (MW)	Production costs ($/H)
			SNEL	NELSAP	Virunga Energie	Nuru			
1.	*Real*	25.713	4	5	19.347	1	93	3.63	5970.74
	Predict	25.752	4.824	5.038	20.055	1.263	25	3.85	6321.84
2.	*Real*	27.427	4	5	21.503	1	90.7	4.07	6508.52
	Predict	27.425	4.666	5.309	22.068	1.395	24	4.26	6885.91
3.	*Real*	28.709	4	5	22	1.901	293.7	4.19	6992.89
	Predict	28.760	4.633	5.507	23.369	1.462	26	4.53	7250.59
4.	*Real*	29.572	4	5	22	2.783	178	4.21	7345.69
	Predict	29.805	4.599	5.732	24.292	1.493	25	4.74	7508.71
5.	*Real*	30.235	4	5	22	3.464	143.8	4.22	7618.09
	Predict	30.596	4.574	5.902	24.990	1.516	26	4.89	7703.86

Table 7 shows that the predicted outputs, based on the estimated demand, are very close to the results obtained using the classical method applied to measured demands. Regarding losses, those from the predictive method and the classical method are similar, with a maximum deviation of 60 kW. In terms of cost, the artificial intelligence-based method achieves further reductions in production costs but occasionally violates the lower limits of sources with high production costs, such as Virunga Energy and Nuru. Lastly, the computation time for this method is approximately five times faster than that of the classical method.

However, when SNEL and NELSAP are unable to meet the demand, and Virunga Energy alone is insufficient, as shown in Table 8, the losses and production costs are almost double those in Table 7. Additionally, there is a violation of the production limits of SNEL and NELSAP, to the detriment of Nuru. Overall, this evaluation demonstrates that Nuru and Virunga Energy, due to their high production costs, are consistently disadvantaged when SNEL and NELSAP can meet the demand. These sources are only utilized during peak periods or when SNEL and NELSAP production is limited, leading to higher costs and losses.

5. Discussion

This study develops a strategy using neural networks to optimize the optimal allocation of energy demand while reducing losses in the transmission network. An LSTM network predicts electricity demand with high accuracy (maximum error of 1.43%) and estimates future production from solar power plants with a maximum error of 9.9%. Additionally, a multilayer perceptron, trained with data from the classical Kuhn-Tucker method, distributes the demand among production units with 90% accuracy and reduced computation time, outperforming classical methods in speed and simplicity. Applied to the Goma network, this approach unifies costs, enhances flexibility, and improves grid reliability while accounting for the dynamics of demand and production.

Compared to other works, this research stands out for its integration of production unit dynamics. For instance, Mountassir (2018) employed CRBMs to predict demand with similar accuracy but on a smaller scale. For power flow optimization, the results align with those of Miodrag (1996), Naama (2007), and Kadir (2019), who also demonstrated that neural networks can replace classical methods with a slight loss in precision but a substantial gain in speed. However, this study goes further by proposing an optimal allocation over a sequence of several hours, anticipating events and enabling more reliable decisions. Despite limitations in technological infrastructure, this research paves the way for the development of smart grids and advanced management systems in electrical networks.

6. Conclusion

This study highlights the potential of Artificial Neural Networks in optimizing energy distribution in Goma. By integrating advanced forecasting models and interconnection networks, the approach achieves higher accuracy and faster computation times compared to classical methods. The findings emphasize the need for centralized energy management and infrastructure investments to ensure equitable and sustainable electricity distribution. Future research should explore real-time applications and scalability to other regions.

References

[1] G. Szustak, P. DąbrowskiORCID and W. G. a. Szewczyk, "The Relationship between Energy Production and GDP: Evidence from Selected European Economies," *MDPI*, vol. 15, no. 1, pp. 1-11, 2021.
[2] SNEL-Goma, "Rapport annuel SNEL-Goma," SNEL, Goma, 2018.
[3] G. Sengi and E. Ntagwirumugara, "Improving reliability of the power distribution system in Goma (DRC) using solar distributed generation," *Journal of Energy in Southern Africa*, vol. 32, no. 4, pp. 84-101, 2021.
[4] M. Djukanovic, M. Calovic, B. Milosevic and D. Sobajic, "Neural-net based real-time economic dispatch for thermal power plants," *IEEE*, vol. 11, no. 4, pp. 755 - 761, 1996.
[5] J. Kumar and G. Sheble, "Clamped state solution of artificial neural network for real-time economic dispatch," *IEEE*, vol. 10, no. 2, pp. 925-931, 2002.
[6] B.Naama, H.Bouzeboudja, Y.Remdani and A.Chaker, "Optimisation des Puissances dans un Réseau d'Energie Electrique par L'Intelligence Artificielle," *International Conference on Computer Integrated Manufacturing*, vol. 4, 2017.
[7] M. Syai'in and A. Soeprijanto, "Neural Network Optimal Power Flow (NN-OPF) based on IPSO with Developed Load Cluster Method," *International Journal of Electrical, Computer, Energetic, Electronic and Communication Engineering*, vol. 4, no. 12, pp. 1701-1706, 2010.
[8] F. Mountassir, "Machine Learning au service de la prédiction de la demande d'énergie dans les Smart Grid," *Mediterranean Telecommunications Journal* , vol. 8, no. 2, 2018.
[9] K. ABACI and V. YAMAÇLI, "Hybrid Artificial Neural Network by Using Differential Search Algorithm for Solving Power Flow Problem," *Advances in Electrical and Computer Engineering*, vol. 19, no. 4, pp. 57-64, 2019.
[10] A. CIZA, C. MICHELLIER, K. KARUME and F. KERVYN, "Vulnerability of the water and the electricity distibution networks in Goma city, facing the lava flows of Nyiragongo volcano (DR Congo)," *Geo-Eco-Trop*, vol. 2, no. 41, pp. 293-312, 2017.
[11] H. Saadat, Power System Analysis, New York: McGraw-Hill, 1999.
[12] Imdadullah, B. Alamri, M. A. Hossain and M. S. J. Asghar, "Electric Power Network Interconnection: A Review on Current Status, Future Prospects and Research Direction," *Electronics MDPI*, vol. 10, no. 2179, 2021.
[13] MIRCEA, C.-C. L. and A.-A. E., Advanced Solutions in power systems, Canada: The Institute of Electrical and Electronics Engineers, 2016.
[14] B. F. W. G. B. S. Allen J. Wood, Power generation, operation, and control third edition, Canada: IEEE Willy, 2014.
[15] Y. Yong, S. Xiaosheng, H. Changhua, Zhang and Jianxun, "AReview of Recurrent Neural Networks: LSTMCells and Network Architectures," *Neural Computation*, vol. 31, p. 1235–1270, 2019.
[16] M. C. Popescu, V. E. Balas, L. P. Popescu and N. Mastorakis, "Multilayer Perceptron and Neural Networks," *WSEAS TRANSACTIONS on CIRCUITS and SYSTEMS*, vol. 8, no. 7, pp. 579-588, 2009.
[17] World Bank, Increasing access to electricity in the Democratic Republic of Congo. Opportunities and challenges, Washington, DC: World Bank, 2020.
[18] V. Energie, "Crédit d'électricite," Goma, 2024.

Author Profile

MSc. KAMBALE PAWASE Gershome is currently a teaching assistant and research laboratory manager in the Department of Science and Technology at Sapientia Catholic University of Goma. From 2016 to 2021, he pursued his undergraduate studies at Sapientia Catholic University of Goma (SCU-Goma), in the Faculty of Applied Sciences, specializing in Electrical Engineering with a focus on Power Engineering. In 2019, he became a member of SCU-Goma-Innovation and was one of the key contributors to the design of DIDA (Intelligent Automatic Disinfection Device) to combat the spread of COVID-19. In 2023, he earned his master's degree in Electrical Engineering, specializing in Power Engineering, also from Sapientia Catholic University of Goma.